Available online at www.sciencedirect.com

ScienceDirect

IFAC Papers Online CONFERENCE PAPER ARCHIVE

IFAC PapersOnLine 56-2 (2023) 11267–11272

Performance Analysis of eXogenous Kalman Filter for INS/GNSS Navigation Solutions

Mushfiqul Alam*. James Whidborne. * and Murat Millidere*

*School of Aerospace Transport and Manufacturing, Cranfield University, MK430AL United Kingdom (Tel: +44 (0) 1234 75 4494; e-mail: mushfiqul.alam@cranfield.ac.uk).

There are several methods of fusing data for navigation solutions using Inertial Navigation System (INS) aided by Global Navigation Satellite System (GNSS). The most used solutions are nonlinear observer (NLO) and extended Kalman filter (EKF) of various architectures. EKF based estimation methods guarantees sub-optimal solutions but not stability, on the contrary NLO based estimation guarantees stability but not optimality. These complimentary features of EKF and NLO has been combined to design an eXogenous Kalman filter (XKF) where the estimate from the NLO is used as an exogenous signal to calculate the linearized model of the EKF. The performance of the designed XKF is tested on real flight test data collected using a Slingsby T67C ultra-light aircraft. The results show that during the outage of GNSS, in some cases the divergence of position estimates using XKF is lower compared to EKF and NLO, however no clear benefit is achieved.

Keywords: INS, GNSS, localization, navigation, Kalman filer, nonlinear observer, eXogenous Kalman filter,

1. INTRODUCTION

MEMS (Micro-Electro-Mechanical System) based inertial measurement unit (IMU) consisting of consisting of tri-axial accelerometer (ACC) angular rate sensor (ARS) aided with GNSS (Global Navigation Satellite System) has been a popular choice for localization of a dynamic vehicle due its cost effectiveness. For a strapdown navigation solution, data fusion techniques can be applied for the estimation of position, velocity, and attitude (PVA) e.g., Rohac et al., 2017.

There are several methods of fusing INS/GNSS in order to obtain PVA estimates, such as temporally interconnected observers, e.g. Bristeau and Petit, 2011, complementary filters or Kalman filters (KF) with various architectures e.g. Alam et al., 2016; Farrell, 2008; Simon, 2010, nonlinear observers (NLO) e.g. Fourati and Belkhiat, 2016, unscented Kalman filters (UKF) and particle filters (PF) e.g. Gustafsson et al., 2002. Due to the dynamic motion of most vehicles being highly nonlinear, the most used approaches to estimate PVA in real-time utilizes nonlinear observers (NLO) and extended Kalman filter (EKF).

The KF or its nonlinear variant EKF generally provide a recursive globally optimal (for the case of KF) or sub-optimal (for the case of EKF) estimate in terms of minimum error variance, e.g., Bar-Shalom et al., 2001. It is an established state estimation method for a linear or nonlinear state space model which assumes that the inputs have normal distribution and characterized by their mean and covariance values. The shortfall of the KF (and EKF) is computation of the inverse covariance matrix of the measurement vector due to round-off errors when implemented into microcontrollers and its high computational cost. In addition, for the case of EKF when approximate linearization is applied, the solution is sub-optimal and global stability cannot be guaranteed in general, and existing stability analysis gives implicit conditions that cannot be verified before as they depend on initial errors and system trajectories e.g., Reif et al., 1998.

On the other hand, NLOs are based on a deterministic approach, unlike the stochastic approach of the KFs/EKFs, motivated by the higher computational load. NLOs usually take global asymptotic or exponential stability (or at least a large region of attraction) as the primary starting point for the design, and then employ tuning parameters to pursue desired performance. In comparison when designing EKFs, the stability properties is determined explicitly due to no stability guarantee for nonlinear systems.

Combining the property of EKFs providing estimates that are sub-optimal and NLOs providing estimates that are guaranteed globally stable, a two-stage estimator called eXogeneous Kalman Filter (XKF) has been proposed recently e.g., Johansen and Fossen, 2017. Within the XKF, the NLO and EKF are cascaded where the estimate from the nonlinear observer is fed as an exogenous signal only used for generating a linearised model to the EKF. It was shown that the estimates from XKF inherits the global stability property of the NLOs, and sub-optimal properties EKF can be achieved, see e.g., Johansen and Fossen, 2017.

The purpose of the paper is to design and develop a data fusion technique for navigation data estimates (PVA estimates) using eXogeneous Kalman Filter estimation architecture and study the performance analysis for INS/GNSS navigation solutions from a real flight test data collected using a dynamic ultra-light Slingsby T67C aircraft. Rest of the paper is organised as follows, Section 2 outlines the design and development of XKF in addition to the design of a NLO and EKF. Section 3 presents the experimental set-up, INS sensors used for data collection and flight trajectory. Section 4 presents the results on the performance analysis of the XKF. Section 5 finally concludes the paper with final remarks.

10.1016/j.ifacol.2023.10.319

2. DESIGN OF XKF

This section outlines the design of NLO and EKF followed by the design of XKF.

2.1 NONLINEAR OBSERVER (NLO)

The kinematic equations describing position p^e, linear velocity v^e, attitude q_b^e, and ARS bias b^b are given as:

$$\begin{aligned}\dot{p}^e &= v^e,\\ \dot{v}^e &= -2\,S(\omega_{ie}^e)\,v^e + f^e + g^e(p^e),\\ \dot{q}_b^e &= \frac{1}{2}q_b^e \otimes \bar{\omega}_{ib}^b - \frac{1}{2}\bar{\omega}_{ie}^e \otimes q_b^e,\\ \dot{b}^b &= 0,\\ \dot{b}_f^b &= 0.\end{aligned} \tag{1}$$

Subscript e is defined in Earth-Centered-Earth-Fixed coordinate frame and subscript b is defined in Body frame. The position and velocity are given in the ECEF-frame, while the ARS bias is in the Body-frame (BF), and the attitude is expressed as a unit quaternion describing the rotation between BF and ECEF. Here the skew-symmetric matrix $S(\cdot)$ is such that the vector product is; $x_1 \times x_2 = S(x_1)x_2$. The gravity vector, $g^e(\cdot)$, is assumed known for a given position, while a vector $x \in \mathbb{R}^3$ can be represented as a quaternion with zero real part and vector part x, i.e. $\bar{x} = [0; x]$. The Earth rotation, ω_{ie}^e, is constant and known, and the product of two quaternions, q_1 and q_2, is given as $q_1 \otimes q_2$. The ARS bias, b^b, and ACC bias, b_f^b, are slowly time-varying.

2.1.1 Nonlinear GNSS/INS Integration

The nonlinear observer structure consists of two parts: an attitude estimator and a translational motion observer (TMO). The attitude estimator determines the vehicle attitude from inertial measurements, whereas the translational motion observer utilizes global measurements provided by a GNSS receiver as well as specific force measurements.
An estimate of the specific force in the ECEF is fed back from the TMO to the attitude estimator, making the structure a feedback interconnection of two subsystems. The observer structure was shown to be semi-globally stable, see e.g., Grip et al., 2015.

2.1.2 Attitude Estimation

The vehicle attitude is represented by a unit quaternion, $\hat{q}_b^e$, describing the rotation from BF to ECEF. Furthermore, the attitude estimator also determines a ARS bias estimate, $\hat{b}^b$, to compensate for sensor drift. The attitude estimation is given by

$$\begin{aligned}\dot{\hat{q}}_b^e &= \frac{1}{2}\hat{q}_b^e \otimes \left(\bar{\omega}_{ib,IMU}^b - \bar{\hat{b}}^b + \bar{\hat{\sigma}}\right) - \frac{1}{2}\bar{\omega}_{ie}^e \otimes \hat{q}_b^e,\\ \dot{\hat{b}}^b &= \mathrm{Proj}\left(-k_I\hat{\sigma}, \left\|\hat{b}^b\right\|_2 \le M_{\hat{b}}\right).\end{aligned} \tag{2}$$

Here the projection function, $\mathrm{Proj}(\cdot,\cdot)$, limits the ARS bias estimate to be within a sphere of radius $M_{\hat{b}}$, where k_I is a constant gain and $\hat{\sigma}$ is an injection term. The injection term is based on the comparison of two vectors in the BF, $\underline{v_1^b}$ and $\underline{v_2^b}$, with two corresponding vectors in the ECEF, $\underline{v_1^e}$ and $\underline{v_2^e}$:

$$\hat{\sigma} = k_1\underline{v_1^b} \times R(\hat{q}_b^e)^T\underline{v_1^e} + k_2\underline{v_2^b} \times R(\hat{q}_b^e)^T\underline{v_2^e}.$$

The gains, k_1 and k_2, are positive and sufficiently large tuning constants. The vectors can be chosen in various ways utilizing e.g., magnetometer or pressure measurements. Here the vectors are chosen, based on specific force and heading from the GNSS velocity, as:

$$\begin{aligned}\underline{v_1^b} &= \frac{f_{IMU}^b}{\left\|f_{IMU}^b\right\|_2}, \quad \underline{v_1^e} = \frac{\hat{f}^e}{\left\|\hat{f}^e\right\|_2}\\ \underline{v_2^b} &= \begin{bmatrix}\cos(\chi)\\ -\sin(\chi)\\ 0\end{bmatrix}, \quad \underline{v_2^e} = R_n^e\begin{bmatrix}1\\0\\0\end{bmatrix}\end{aligned} \tag{3}$$

where the specific force estimate, $\hat{f}^e$, is determined by the translational motion observer. The reference vector $\underline{v_2^e}$ denotes the direction North decomposed in the ECEF frame, while the corresponding body vector, $\underline{v_2^b}$, utilizes the course angle χ. The course angle can be obtained from a compass or in this case from GNSS velocity measurements in NED frame:

$$\chi = \tan^{-1}\left(\frac{v_e}{v_n}\right),$$

where v_n and v_e signifies the velocity in North and East direction.

2.1.3 Accelerometer Bias Estimation

The bias of the ACC measurements can be considered a slowly time-varying value added to the true measurements; $f_{IMU}^b = f^b + b_f^b$. Considering a combination of parameters $\theta = \left[\left\|\hat{b}_f^b\right\|_2, \left(\hat{b}_f^b\right)^T\right]^T$ and $\phi = [1, -2(f_{IMU}^b)^T]^T$ the measurement for the injection term can be expressed as $y_f = \left\|\hat{b}_f^b\right\|_2 - 2(f_{IMU}^b)^T\hat{b}_f^b$. The combination vector propagation is then expressed as:

$$\dot{\hat{\theta}} = \Gamma\phi\left(y_f - \phi^T\hat{\theta}\right),$$

where Γ is a positive-definite symmetric gain matrix. The ACC bias is carried out under the assumption that there is sufficient excitation of the vehicle for the ACC to experience versatile acceleration. Formally this requirement is expressed as an assumption that:

$$\int_t^{t+T}\phi(\tau)\phi^T(\tau)d\tau \ge \epsilon I,$$

where $\epsilon > 0$ and $T > 0$ such that for each $t \ge 0$ the condition is satisfied and the persistently excitation assumption is valid. The ACC bias estimation can be implemented similarly to the ARS bias estimation,

$$\dot{\hat{\theta}} = \mathrm{Proj}\left(\Gamma\phi\left(\hat{y}_f - \phi^T\hat{\theta}\right), \left\|\hat{\theta}\right\|_2 \le M_{\hat{w}}\right),$$

where $M_{\hat{w}}$ is a bound on the length of the bias vector.

2.1.4 Translational Motion Observer

The translational motion observer (TMO) estimates position, linear velocity, and specific force of the vehicle by

using injection terms based on the difference in measured and estimated global position. A GNSS receiver provides the global position measurements. The TMO is given as:

$$\dot{\hat{p}}^e = \hat{v}^e + \theta K_{pp}(p^e_{GNSS} - \hat{p}^e) + K_{pv}(v^e_{GNSS} - C_v\hat{v}^e),$$

$$\dot{\hat{v}}^e = -2S(\omega^e_{ie})\hat{v}^e + \hat{f}^e + g^e(\hat{p}^e) + \theta^2 K_{vp}(p^e_{GNSS} - \hat{p}^e) + \theta K_{vv}(v^e_{GNSS} - C_v\hat{v}^e),$$

$$\dot{\xi} = -R(\hat{q}^e_b)S(\hat{\sigma})f^b_{IMU} + \theta^3 K_{\xi p}(p^e_{GNSS} - \hat{p}^e) + \theta^2 K_{\xi v}(v^e_{GNSS} - C_v\hat{v}^e),$$

$$\hat{f}^e = R(\hat{q}^e_b)(f^b_{IMU} - b^b_f) + \xi.$$

Here an auxiliary state, ξ, has been introduced for estimation of the specific force. The tuning parameter θ is typically chosen to be equal to 1. The additional injection term based on linear velocity measurements and estimates was shown in e.g., Grip et al., 2012, not to be essential to the observer stability, however, it does increase performance. Hence the matrix C_v can be chosen to be zero.

Introducing the error variables; $\tilde{p} = p^e - \hat{p}^e$, $\tilde{v} = v^e - \hat{v}^e$, and $\tilde{f} = f^e - \hat{f}^e$, the state vector of the error dynamics can be stated as $\tilde{x} = [\tilde{p}; \tilde{v}; \tilde{f}]$. The gains of the translational motion observer can then be chosen to satisfy $A - KC$ being stable. The gains can be chosen to be constant without issue to the stability of the observer. Details of the gain calculation can be found in e.g., Rohac et al., 2017.

2.2 EXTENDED KALMAN FILTER (EKF)

This section describes the details of a two stage EKF for the navigation data estimation. The overall estimation process is divided into two main sections: an Attitude estimator and a Position/Velocity estimator. The details of the estimation can be found in e.g., Rohac et al., 2017.

In the following sections, each part of the estimator structure will be introduced in detail.

2.2.1 EKF based Attitude Estimator

The vehicle attitude is represented in this case by Euler angles since we assume singularity free calculations. This assumption comes from the operation conditions and limits of any aircraft. The state vector, $\boldsymbol{x}$ is updated via a transition function (4) and (5) when angular rates form a control vector. Expected measurements (6) are related to ACC readings when only gravity affects the sensor, which means non dynamic motion.

$$\begin{aligned} &\hat{\boldsymbol{x}} = \begin{bmatrix}\hat{\boldsymbol{\theta}} & \hat{\boldsymbol{b}}_g\end{bmatrix}^T, \\ &\boldsymbol{u} = \omega^b_{ib} = \begin{bmatrix}\omega_{b_x}, \omega_{b_y}, \omega_{b_z}\end{bmatrix}^T \end{aligned} \tag{4}$$

$$\boldsymbol{x_{k+1}} = \boldsymbol{x_k} + T \times \begin{bmatrix} \begin{bmatrix} 1 & \sin\phi\tan\theta & \cos\phi\tan\theta \\ 0 & \cos\phi & -\sin\phi \\ 0 & \sin\phi\sec\theta & \cos\phi\sec\theta \end{bmatrix} \left(\begin{bmatrix}\omega_{b_x} \\ \omega_{b_y} \\ \omega_{b_z}\end{bmatrix} - \begin{bmatrix}b_{g_x} \\ b_{g_y} \\ b_{g_z}\end{bmatrix} \right) \\ 0 \\ 0 \\ 0 \end{bmatrix} \tag{5}$$

$$\boldsymbol{z} = \begin{bmatrix} f_x \\ f_y \\ f_z \\ \psi_{GNSS} \end{bmatrix}, \hat{\boldsymbol{z}}_{\boldsymbol{k}} = \begin{bmatrix} sin\theta \\ -cos\theta sin\phi \\ -cos\phi sin\theta \\ \psi \end{bmatrix} \tag{6}$$

The heading (ψ) is evaluated based on the GNSS velocities. The detailed condition for using the GNSS velocities for the estimation of heading angle can be found in e.g., Rohac et al., 2017.

2.2.2 EKF based Position/Velocity Estimator

The position estimation is made in NED frame, velocity in the body-frame and ACC bias of the vehicles while using GNSS position and velocity as aiding measurements. The state vector (7) is updated via the transition function (9) where the control vector $\boldsymbol{u}$ (8) contains ACC measurements in terms of a specific force, Euler angles and anti-centrifugal force (ACF). The measurement vector (10) contains position estimates from GNSS and downward velocity in body axis. The estimation equations are given as:

$$\hat{\boldsymbol{x}} = \begin{bmatrix}\hat{\boldsymbol{p}}_{\boldsymbol{n}} & \hat{\boldsymbol{v}}_{\boldsymbol{b}} & \hat{\boldsymbol{b}}_{\boldsymbol{a}}\end{bmatrix}^T \tag{7}$$

$$\boldsymbol{u} = [\, \boldsymbol{f}^b, \quad \boldsymbol{\theta}, \quad \boldsymbol{ACF}\,]^T \tag{8}$$

$$x_{k+1} = x_k + T \times \begin{bmatrix} C^n_b \begin{bmatrix}U \\ V \\ W\end{bmatrix} \\ C^{n^T}_b \begin{bmatrix}0 \\ 0 \\ g\end{bmatrix} + \left(\begin{bmatrix}SF_x \\ SF_y \\ SF_z\end{bmatrix} - \begin{bmatrix}b_{ax} \\ b_{ay} \\ b_{az}\end{bmatrix} \right) - ACF \\ 0 \\ 0 \\ 0 \end{bmatrix}, \tag{9}$$

$$z = \begin{bmatrix}\boldsymbol{p^n_{GNSS}} \\ v^b_{GNSS}\end{bmatrix}, \; \hat{z}_k = \begin{bmatrix}\hat{\boldsymbol{p}}_{\boldsymbol{n}} \\ \hat{v}^b_{Down}\end{bmatrix}. \tag{10}$$

The ACF is the anti-centrifugal force calculation can be found in e.g., Rohac et al., 2017.

2.3 Design of The Exogenous Kalman Filter

The XKF is implemented in combination of the already designed NLO and EKF. The Jacobian or the linearization of the EKF's of Eq (5) and Eq (9) to calculate the transition matrix is performed based on the estimated states by NLO. The details of the block diagram for XKF can be found in e.g., Johansen & Fossen, 2017. The tuning values of the NLO and EKF can be found in e.g., Rohac et al., 2017.

3. EXPERIMENTAL SETUP

The flight experiment was conducted using a Slingsby T67C aircraft (General Aviation category), shown in Fig. 1a. To obtain GNSS data and inertial data, a DMU-10 (Silicon Sensing) IMU was used which was connected with a MAX8W (μBlox) GNSS receiver. The DMU-10 is of commercial grade with 6 degree of freedom MEMS based IMU consisting of 3

gyros, 3 ACCs and a temperature sensor. The data from the GNSS receiver and DMU-10 were pooled by a microcontroller STM32F746ZGT6 (STMicroeletcronics). The data from the IMU and GNSS receiver were sampled at 200 Hz and 5 Hz respectively.

(a)

(b)

Fig. 1. Slingsby T67C aircraft (a), the sensory compartment inside Pelicase 1450 (b).

The data from an X91+ GNSS receiver were sampled at 5 Hz and were related to measurements obtained from GNSS stationary reference station placed in Pribram city, which is a part of Czech Reference GNSS Station Network (CZEPOS). The GNSS data were processed in the open source RTKlib to give an accurate RTK-GNSS based position used as a reference (true) data source for this article. The navigation unit was mounted in a sensory compartment inside a Pelicase 1450 as depicted in Fig. 1b and placed onboard the aircraft.

3.1 DESCRIPTION OF EXPERIMENT

The flight included various flight patterns including slow turns and rapid altitude changes, see Fig. 2a. The flight included rapid altitude change from 450 m up to 1040 m and vice-versa. The flight took about 33 minutes including rolling, take-off, climb, cruise, descent, and landing as marked Fig. 2b. Since different stages during the flight had different conditions for the navigation unit to operate, we divided the obtained data according to flight stages and analyzed the navigation solution performance separately in each of them. During the flight, there were conditions with high dynamics reaching angular rates up to ± 50°/s and values of a total acceleration of -5.2 g and +2.3 g.

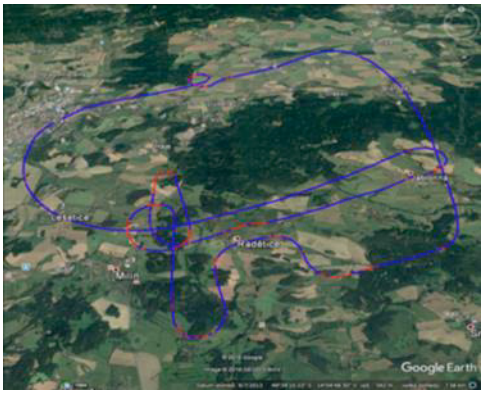

(a)

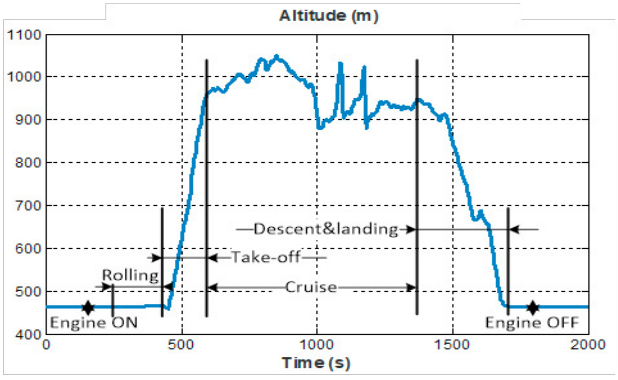

(b)

Fig. 2. 2D trajectory of the flight performed – referential data obtained with RTKlib 2.4.2 with an indicated status of the GNSS receiver (blue – fix, red - float) (a); an altitude profile of the flight with emphasized stages b).

4. PERFORMANCE ANALYSIS

To assess the performance of the XKF with respect to the NLO and EKF, the GNSS aiding data was artificially turned off for 30 seconds in each 5-minute interval; except the first one which was left for initialization of estimating process as shown in Fig. 3 marked in red circles.

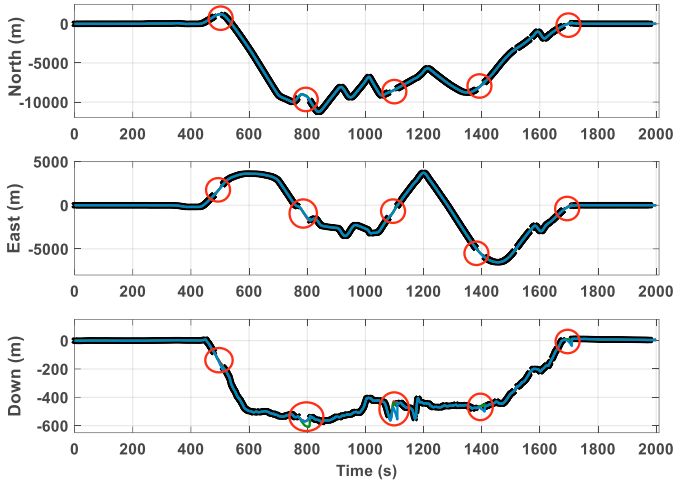

Fig. 3. Positions where the GNSS is artificially turned off.

Three types of estimation are compared with each other as below:

1. Estimation using EKF only
2. Estimation using NLO only
3. Estimation using XKF

Fig. 4 shows the results of the PVA estimations along with the ACC and ARS bias estimates. From the position and velocity plots in Fig. 4c and Fig. 4d the estimates using EKF diverges rapidly when there is no GNSS aiding available. In contrast the estimate using XKF diverges slowly. It is because the bias estimation in the accelerometers is not stabilised by the EKF.

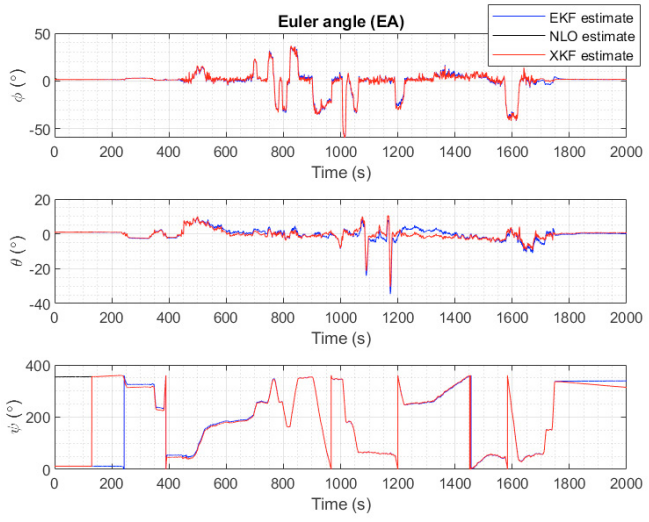

(a) Euler's angle estimation.

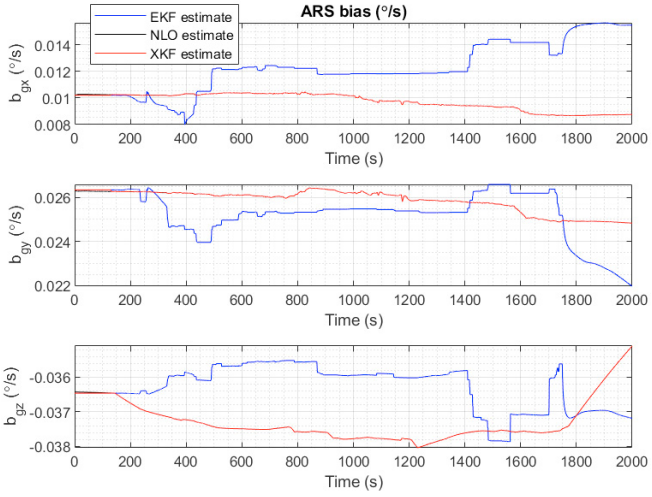

(b) Angular rate sensor's bias estimate.

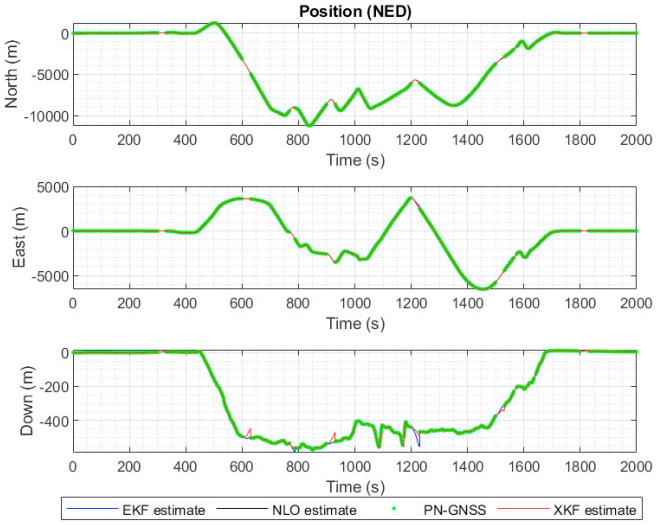

(c) Position estimates.

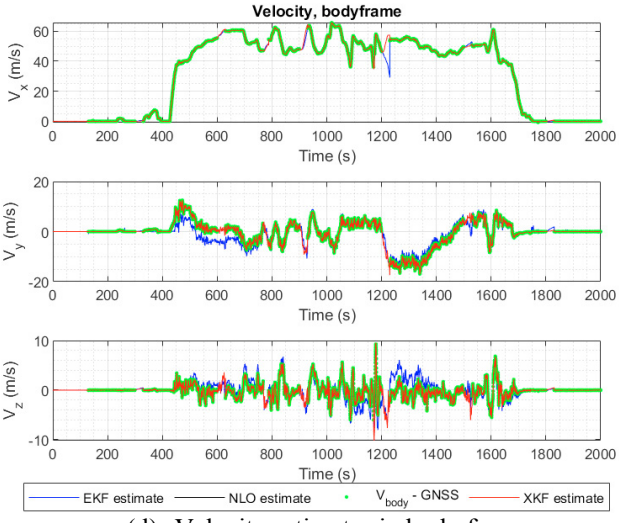

(d) Velocity estimates in body frame.

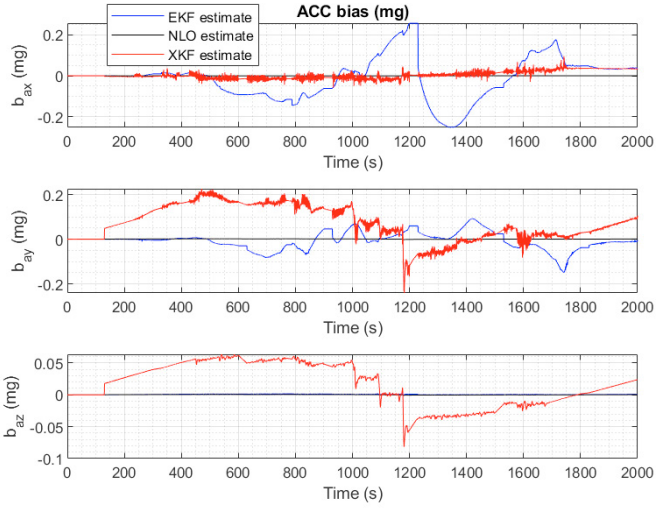

(e) Accelerometer bias estimation.

Fig. 4. PVA estimates using NLO, EKF and XKF.

It can also be seen from that the bias estimates for ACC and ARS Fig. 4b and Fig. 4e varies significantly using EKF compared to the XKF. Bias does not vary as fast as estimated by the EKF; hence it can be said that bias estimation by EKF

is not stabilised. In comparison the bias estimate using XKF is stabilized.

To quantify the results of the estimation during the GNSS outages, RMSE was calculated with respect to the absolute GPS position and velocity. Resultant RSME values in position are summarized in Table 1. In the table green refers to the improvement in performance, amber denotes the moderate performance and red indicates the worse performance in terms of the deviation from the actual position.

Table 1. Resultant RMSE values for NED position estimates during GNSS outages.

Outage Position	RMSE in position – direction North, East, Down								
	North (m)			East (m)			Down (m)		
	EKF	NLO	XKF	EKF	NLO	XKF	EKF	NLO	XKF
1	7.9	15.8	14.1	16.6	12.4	11.4	1.8	25.7	24.7
2	7.5	14.9	14.9	10.4	9.4	9.4	12.1	4.9	4.3
3	6.7	23.5	23.6	28.8	13.1	13.3	31.8	27.6	25.6
4	31.5	15.1	14.3	129.1	22.2	21.4	50.0	18.9	18.2
5	38.2	11.3	11.2	18.4	12.6	11.8	5.4	12.5	12.0

It can be seen in Table 1 that in the easternly and downward direction the XKF always performed better in terms of the reduced divergence from the actual position. In the North direction it is sometimes EKF estimates better and sometime the XKF estimates better. This might be due to the use of heading correction in the EKF using the GNSS velocity. Overall, from the Table 1 it can be said that XKF performs better in situation where there is GNSS outage compared to EKF and NLOs alone. There is not clear evidence that XKF globally improves the performance of the PVA estimates when compared to EKF or NLO.

5. CONCLUSIONS

In this paper the performance of a recently proposed eXogenous Kalman filter (XKF) has been analysed and compared using real flight test data for INS/GNSS based navigation solutions for Position, Velocity and Attitude (PVA) estimates. The performance of the XKF was compared against nonlinear observer (NLO) and two-stage extended Kalman Filter (EKF). For the performance analysis of the XKF, EKF and NLO for navigation data estimation, GNSS outage was artificially created to study which filter diverges the most. It was found that XKF diverges the least in the East and Down position estimation compared to EKF and NLO. On the other hand, the Northern position estimates provided similar performance for using EKF and XKF. Even though no extra benefit was achieved in North position estimate using XKF, it stabilized the bias estimates of the sensors under dynamic conditions. Hence the use of XKF is suitable for PVA estimates.

ACKNOWLEDGMENT

The authors would like to thank Dr. Martin Sipos at the Department of Measurement, Faculty of Electrical Engineering, Czech Technical University in Prague, and Prof. Thor Fossen and Prof Tor Johansen at Norwegian University of Science and Technology for the provision of flight data and collaborative work.

REFERENCES

Alam, M., Moreno, G., Sipos, M. and Rohac, J. (2016), "INS / GNSS Localization Using 15 State Extended Kalman Filter", *International Conference in Aerospace for Young Scientists*, pp. 425–435.

Bar-Shalom, Y., Li, X.-R. and Kirubarajan, T. (2001), *Estimation with Applications to Tracking and Navigation*, John Wiley & Sons, Inc., New York, USA, doi: 10.1002/0471221279.

Bristeau, P.-J. and Petit, N. (2011), "Navigation system for ground vehicles using temporally interconnected observers", *American Control Conference (ACC), 2011*, pp. 1260–1267.

Farrell, J. (2008), *Aided Navigation: GPS with High-Rate Sensors*, McGraw-Hill, Inc.

Fourati, H. and Belkhiat, D.E.C. (2016), "Multisensor attitude estimation: Fundamental concepts and applications", *Multisensor Attitude Estimation: Fundamental Concepts and Applications*, CRC Press, pp. 1–580, doi: 10.1201/9781315368795.

Grip, H.F., Fossen, T.I., Johansen, T.A. and Saberi, A. (2012), "Attitude Estimation Using Biased Gyro and Vector Measurements With Time-Varying Reference Vectors", *IEEE Transactions on Automatic Control*, Vol. 57 No. 5, pp. 1332–1338, doi: 10.1109/TAC.2011.2173415.

Grip, H.F., Fossen, T.I., Johansen, T.A. and Saberi, A. (2015), "Globally exponentially stable attitude and gyro bias estimation with application to GNSS/INS integration", *Automatica*, Vol. 51, pp. 158–166, doi: 10.1016/j.automatica.2014.10.076.

Gustafsson, F., Gunnarsson, F., Bergman, N., Forssell, U., Jansson, J., Karlsson, R. and Nordlund, P.J. (2002), "Particle filters for positioning, navigation, and tracking", *IEEE Transactions on Signal Processing*, Vol. 50 No. 2, pp. 425–437, doi: 10.1109/78.978396.

Johansen, T.A. and Fossen, T.I. (2017), "The eXogenous Kalman Filter (XKF)", *International Journal of Control*, Vol. 90 No. 2, pp. 161–167, doi: 10.1080/00207179.2016.1172390.

Reif, K., Sonnemann, F. and Unbehauen, R. (1998), "An EKF-Based Nonlinear Observer with a Prescribed Degree of Stability", *Automatica*, Pergamon, Vol. 34 No. 9, pp. 1119–1123, doi: 10.1016/S0005-1098(98)00053-3.

Rohac, J., Hansen, J.M.J.M., Alam, M., Sipos, M., Johansen, T.A.T.A. and Fossen, T.I.T.I. (2017), "Validation of nonlinear integrated navigation solutions", *Annual Reviews in Control*, Elsevier, Vol. 43, pp. 91–106, doi: 10.1016/j.arcontrol.2017.03.006.

Simon, D. (2010), "Kalman filtering with state constraints: a survey of linear and nonlinear algorithms", *IET Control Theory & Applications*, Vol. 4 No. 8, p. 1303, doi: 10.1049/iet-cta.2009.0032.

2024-11-22

Performance Analysis of eXogenous Kalman Filter for INS/GNSS Navigation Solutions

Alam, Mushfiqul

Elsevier

Alam M, Whidborne J, Millidere M. (2023) Performance Analysis of eXogenous Kalman Filter for INS/GNSS Navigation Solutions. IFAC-PapersOnLine, Volume 56, Issue 2, pp. 11267-11272. 22nd IFAC World Congress, July 9-14, 2023, Yokohama, Japan

https://doi.org/10.1016/j.ifacol.2023.10.319